

Efficient Neural Network Compression

Hyeji Kim, Muhammad Umar Karim Khan, and Chong-Min Kyung

Korea Advanced Institute of Science and Technology (KAIST), Republic of Korea

{hyejikim89, umar, kyung}@kaist.ac.kr

Abstract

Network compression reduces the computational complexity and memory consumption of deep neural networks by reducing the number of parameters. In SVD-based network compression the right rank needs to be decided for every layer of the network. In this paper we propose an efficient method for obtaining the rank configuration of the whole network. Unlike previous methods which consider each layer separately, our method considers the whole network to choose the right rank configuration. We propose novel accuracy metrics to represent the accuracy and complexity relationship for a given neural network. We use these metrics in a non-iterative fashion to obtain the right rank configuration which satisfies the constraints on FLOPs and memory while maintaining sufficient accuracy. Experiments show that our method provides better compromise between accuracy and computational complexity/memory consumption while performing compression at much higher speed. For VGG-16 our network can reduce the FLOPs by 25% and improve accuracy by 0.7% compared to the baseline, while requiring only 3 minutes on a CPU to search for the right rank configuration. Previously, similar results were achieved in 4 hours with 8 GPUs. The proposed method can be used for lossless compression of a neural network as well. The better accuracy and complexity compromise, as well as the extremely fast speed of our method makes it suitable for neural network compression.

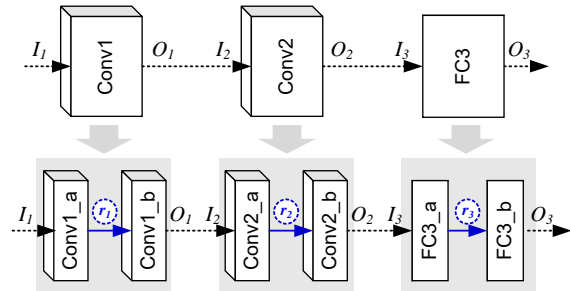


Figure 1. Convolutional and fully-connected layers and their decomposed counterparts. Each layer is split into two with low-rank decomposition.

providing competitive accuracy.

Generally, filter pruning techniques have been used for network compression. The aim of such approaches is to develop pruning policies, which can satisfy the target constraints on FLOPs and memory. Layer wise search-based heuristic methods [11, 18, 23], reinforcement learning [1, 4, 10], and genetic and evolutionary algorithms [22, 25] have been used to define the pruning policy. A greedy selection method based on a heuristic metric has been proposed in [5, 21] to prune multiple filters of the network together.

Another approach towards network compression is using kernel decomposition over each filter in the network. Convolutional and fully connected layers can be represented as matrix multiplications, and kernel decomposition can be applied to these matrices [2, 7, 12, 15, 28]. Kernel decomposition with singular value decomposition (SVD) automatically assigns importance (the singular values) to the decomposed kernels. This automatic sorting makes filter pruning easier, as the decomposed kernels with the lower parameters are the first to be pruned. Simply put, low-rank approximation of a layer decomposes it into two matrix multiplications for network compression as shown in Fig. 1.

With kernel decomposition schemes, the problem boils down to the choice of the optimal compression ratio for each layer of the network. We need to find the right rank configuration (i.e. compression ratios) for the whole network that satisfies constraints on speed, memory and accuracy. This is different from past methods which use a solver to

1. Introduction

Deep convolutional neural networks have been consistently showing outstanding performance in a variety of applications, however, this performance comes at a high computational cost compared to past methods. The millions of parameters of a typical neural network require immense computational power and memory for storage. Thus, model compression is required to reduce the number of parameters of the network. Our aim in this paper is to develop a method that can optimize trained neural networks for reduction in computational power and memory usage while

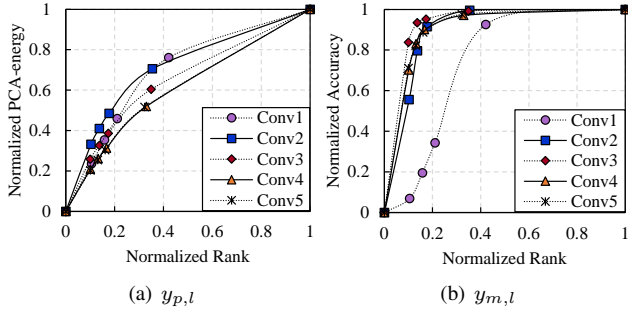


Figure 2. Interpolated function of layer-wise accuracy metric in AlexNet. (a) $y_{p,l}$ based on normalized PCA-energy. (b) $y_{m,l}$ based on normalized accuracy using partial training dataset.

minimize the approximation error at the fixed rank [19, 20] and a training technique to better compensate for accuracy loss [3, 27]. An iterative search-based approach was adopted in [9, 14, 28] to obtain the right rank configuration. In [28], the authors define an PCA energy-based accuracy feature and use it to select a layer to be compressed in every iteration. The final rank of each layer is the result of iterative layer-wise network compression. Reinforcement learning was used in [9] to find the rank of each layer independently. Unlike [28] and [9], which optimize each layer separately, [14] searched for the right rank configuration for the whole network. Although, [14] shows better performance compared to [28] and [9], it still takes significant amount of time due to its iterative search for the right rank configuration.

In this paper, we propose Efficient Neural network Compression (ENC) to obtain the optimal rank configuration for kernel decomposition. The proposed method is non-iterative; therefore, it performs compression much faster compared to numerous recent methods. Specifically, we propose three methods: ENC-Map, ENC-Model and ENC-Inf. ENC-Map uses a mapping function to obtain the right rank configuration from the given constraint on complexity. ENC-Model uses a metric representative of the accuracy of the whole network to find the right rank configuration. ENC-Inf uses both the accuracy model and inference on a validation dataset to arrive at the right rank configuration. The code for our method is available online.¹

The rest of the paper is structured as follows. Section 2 and 3 describe the accuracy metrics. Section 4 discusses ENC-Map. Search-based methods, ENC-Model and ENC-Inf, are given in Section 5. Experiments are discussed in Section 6 and Section 7 concludes the paper.

2. Layer-wise Accuracy Metrics

The error of the neural network can be divided over the constituent layers of the network. In other words, each layer

contributes to the error or accuracy of the neural network. In this section, we describe a couple of metrics, which represents the accuracy contributed by a layer as a function of the rank of that layer. This layer-wise accuracy metrics can be used to predict the contribution of an individual layer to the overall accuracy of the network. The first metric is based on heuristics while the second involves computing the accuracy over a validation dataset.

PCA energy-based Metric. After singular value decomposition (SVD), the number of principal components retained directly affects the complexity as well as the accuracy. The un-normalized PCA energy is given by $\sigma'_l(r_l) = \sum_{d=1}^{r_l} \sigma_l(d)$, where r_l is the rank of the l -th layer in the neural network and $\sigma_l(d)$ is the d -th singular value after performing SVD on the parameters on l -th layer. In detail, $\sigma'_l(r_l)$ is the sum of the first r_l diagonal entries of the diagonal matrix after decomposition. It is obvious that the accuracy decreases with the decrease in un-normalized PCA energy. The PCA energy of the l -th layer with a rank r_l is obtained by performing min-max normalization to the un-normalized PCA energy, i.e.,

$$y_{p,l}(r_l) = \frac{\sigma'_l(r_l) - \sigma'_l(1)}{\sigma'_l(r_l^{max}) - \sigma'_l(1)}. \quad (1)$$

Here r_l^{max} is the maximum or initial rank.

Measurement-based Metric. The second metric for layer-wise accuracy that we use in this paper is based on evaluation of the neural network on a validation dataset. For the l -th layer, the accuracy model is obtained by changing r_l while keeping the rest of the network unchanged. Empirical models are developed for each layer. Note that the possible number of ranks for a layer occupies a large linear discrete space, making it impractical to evaluate the accuracy over the validation dataset. Therefore, we use VBMF [24] to sample ranks over which the accuracy is estimated, and the ranks are sampled to increase the measured accuracy. Then, we follow it up by Piecewise Cubic Hermite Interpolating Polynomial (PCHIP) algorithm. We denote the measurement-based layer-wise accuracy metric of the l -th layer by $y_{m,l}(r_l)$.

In Fig. 2, we show the result of interpolation with both the PCA energy-based and measurement-based approaches. Both the metrics show different profiles. This is because the PCA energy is not a representation of accuracy in itself but monotonic with the overall accuracy.

3. Accuracy Metric

In this section, we describe how we can use the layer-wise metrics to represent the accuracy of the complete neural network. We estimate the joint distribution of the output of the neural network and the configuration of its layers. The configuration of the layers of a neural network is defined only by the choice of the rank for each layer.

¹<https://github.com/Hyeji-Kim/ENC>

Our aim is to maximize the accuracy of the network with a given set of constraints. Let us define the configuration of a neural network through the rank configuration, which is a set of ranks of each layer, i.e.,

$$R = \{r_1, r_2, \dots, r_L\}, \quad (2)$$

where r_l is the rank of the l -th layer. The overall accuracy of the network can be represented by the joint distribution of accuracy of individual layers. Precisely,

$$P(A; R) = P(a_1, a_2, \dots, a_L; R), \quad (3)$$

where a_l is the accuracy provided by the l -th layer. Practically, the accuracy contribution of a layer also depends on the ranks of other layers. However, the accuracy model can be simplified as the function of layer-wise accuracy metric contribution of a layer by applying the layer-wise accuracy metrics in Sec. 2, $y_{p,l}(r_l)$ and $y_{m,l}(r_l)$, which depend on the rank of the layer only. Considering the independence, we can model the overall accuracy metric as

$$P(A; R) = \prod_{l=1}^L P(a_l; r_l). \quad (4)$$

This representation has been inspired by [28] where the product of layer-wise accuracy metrics is used to estimate the overall accuracy.

To estimate the accuracy, we define three types of overall accuracy metric; measurement-based $A_m(R)$, PCA energy-based $A_p(R)$, and the combination of two metrics, $A_c(R)$. The layer-wise metric based on the measured accuracy can be directly used to replace $P(a_l; r_l)$, i.e.,

$$A_m(R) = \prod_{l=1}^L y_{m,l}(r_l). \quad (5)$$

Although the normalized PCA energy of (1) is not defined from the accuracy, it was shown in [28] that the PCA energy of a layer is proportional to the accuracy of the network, allowing us to use the PCA energy as the accuracy metric. Thus, we define the PCA energy-based accuracy metric as

$$A_p(R) = \prod_{l=1}^L y_{p,l}(r_l). \quad (6)$$

In our experiments, we have noticed that the PCA energy metric does not accurately represent the accuracy at very low complexity. Also, as the network is redundant, the measurement-based metric can not sufficiently represent the effect of complexity reduction against accuracy at higher complexities. Therefore, we define a combined metric. This metric takes into consideration both the PCA energy and the measurement based layer-wise accuracy metrics. We have

weighted the PCA energy only with the network complexity to reduce the influence of the $A_p(R)$ at lower complexities and the $A_m(R)$ at higher complexities. Mathematically,

$$A_c(R) = \left\{ A_p(R) \times \frac{C(R)}{C_{orig}} \right\} + A_m(R), \quad (7)$$

where $C(R)$ is the complexity of the rank configuration R and C_{orig} is the total complexity of the network. The complexity $C(R)$ is defined by

$$C(R) = \sum_{l=1}^L C_l(r_l) = \sum_{l=1}^L c_l r_l, \quad (8)$$

where $C_l(r_l)$ is the complexity of the l -th layer. The complexity coefficient c_l for spatial [12] and channel [7] decomposition is $c_l = W_l H_l D_l (I_l + O_l)$ and $c_l = W_l H_l (I_l D_l^2 + O_l)$, respectively. Here W_l and H_l are the width and height of output feature map, D_l is the size of filter window, I_l and O_l are the number of input channels and filters.

As will be seen shortly, we are not interested in the exact value of the estimated accuracy but rather the relative value of accuracy metric obtained from the various rank configurations. In other words, we use the accuracy metric to extract some partial rank configurations with the largest value of accuracy metric.

4. ENC-Map: Rank Configuration with Accuracy-Complexity Mapping

In this section, we present a simple method to choose the rank configuration for a neural network by mapping complexity against accuracy. The mapping is performed through the rank configurations, as both complexity and accuracy are functions of rank configurations. At first, we intuitively thought that all layers having same accuracy penalty would be better compression strategy than having same compression ratio (i.e. uniform). Therefore, we only consider the rank configurations for which layer-wise metrics are equal for every layer. Mathematically,

$$R_e = R \mid y_{i,l}(r_l) = y_{i,k}(r_k), \quad (9)$$

where $l, k \in 1, 2, \dots, L$ and $i \in \{p, m\}$. Next the complexity of R_e , $C(R_e)$, is computed using (8). The accuracy metric and complexity are plotted against each other over R_e , which provides a mapping between complexity and accuracy metric. The mapping is mathematically given as

$$f_{C-A} : \mathbb{R} \rightarrow \mathbb{R}. \quad (10)$$

Also note that the mappings from complexity and accuracy metric to the rank configuration and vice versa do exist as well, i.e.,

$$f_{C-R} : \mathbb{R} \rightarrow \mathbb{R}^L. \quad (11)$$

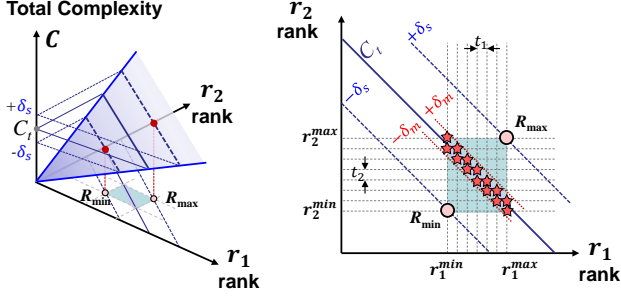


Figure 3. Extraction of candidate rank configurations (as an example of two-layered CNN). The effective space is defined by boundaries of rank configuration, R_{max} and R_{min} , and step size t_1 , where the complexity is around target complexity C_t with space margin $\pm\delta_s$. The candidate rank configurations are lying on C_t with the complexity margin $\pm\delta_m$ denoted as star points.

Using this mapping, the respective rank configuration is calculated from the inverse function of layer-wise accuracy metric, where $a = y_{k,l}(r_l)$ is converted to $r_l = y_{k,l}^{-1}(a)$ and $k \in \{p, m\}$. Note that the inverse exists as $y_{k,l}(r_l)$ is an increasing function as shown in Fig. 2. Here, a is the achievable layer-wise accuracy metric obtained from f_{C-A} , while satisfying constraints on complexity. This method is called ENC-Map as we use a simple mapping to obtain the right rank configuration.

5. ENC-Model/Inf: Rank Configuration in Combinatorial Space

The method described in the previous section strongly depends on the equal layer-wise metrics. Therefore, we extend the rank configuration to the combinatorial problem to choose the optimal rank configuration in the non-equal layer-wise metrics.

The combinatorial space is defined by the Cartesian product of the vector space of rank for each layer. In this space, we extract the partial rank configurations that satisfy the target complexity called candidate rank configurations as illustrated in Fig. 3. To quickly extract the candidate rank configurations and find the optimal rank configuration in non-iterative manner, we perform two steps. First, we limit the range of the ranks with ENC-Map. Then, we extract the candidate rank configurations by hierarchically grouping the layers to reduce the number of effective layers for sub-space generation.

5.1. Limiting the Search Space

To limit the search space, we use the simple method described in the previous section. We obtain the upper and lower bounds on the search space near the target complexity by using the mapping in (11) by

$$R_{max} = f_{C-R}(C_t + \delta_s), \quad (12)$$

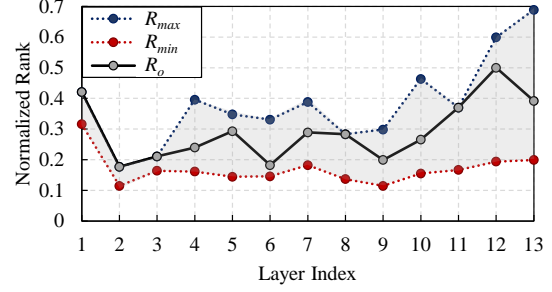


Figure 4. Distribution of normalized rank configurations for VGG-16 ($C_t=25\%$, $\delta_s=10\%$). A final rank configuration R_o is selected within the boundaries, $R_{max}(C=35\%)$ and $R_{min}(C=15\%)$.

$$R_{min} = f_{C-R}(C_t - \delta_s). \quad (13)$$

Here C_t is the complexity constraint and δ_s is the space margin. The final rank configuration, R_o , is defined within the space boundaries, R_{max} and R_{min} , as shown in Fig. 4.

5.2. Min-offsetting the Search Space

In the limited space by the R_{max} and R_{min} , we are only interested in the candidate rank configurations \mathbf{R} as

$$\mathbf{R} = \bigcup R \mid C_t - \delta_m < C(R) < C_t + \delta_m, \quad (14)$$

for $R \in [R_{min}, R_{max}]$. \mathbf{R} includes the rank configurations for which the complexity is roughly equal to C_t . Note that we slightly expand the search space by using the parameter δ_m . To simplify the computations, we shift the space boundaries from $[R_{min}, R_{max}]$ to $[0, R_{max} - R_{min}]$. Then, we generate the differential search space and extract the differential candidate rank configurations $\hat{\mathbf{R}}$ defined by

$$\hat{\mathbf{R}} = \bigcup R \mid \Delta C_t - \delta_m < C(R) < \Delta C_t + \delta_m, \quad (15)$$

for $\Delta C_t = C(R_{max}) - C_t$ and $R \in [0, R_{max} - R_{min}]$. Note that $\mathbf{R} = R_{max} - \hat{\mathbf{R}}$.

5.3. Hierarchical Extraction of $\hat{\mathbf{R}}$

It is not feasible to generate the complete combinatorial search space for deep neural network, since the space complexity is exponential to the number of layers. Hence, we hierarchically generate the sub-spaces by grouping some layers in a top-down manner as illustrated in Fig. 5 and extract the candidate rank configurations.

As denoted in (8), the complexity is the weighted sum of the complexity coefficient and rank of each layer. From the min-offset space, layers having same complexity coefficient c_i can simply be grouped from $\{r_i, r_{i+1}, r_{i+2}, \dots\}$ to r'_i . The groped rank r'_i is defined by

$$r'_i = [0 : \min(\{t_i\}) : \sum \{max(r_i)\}], \quad (16)$$

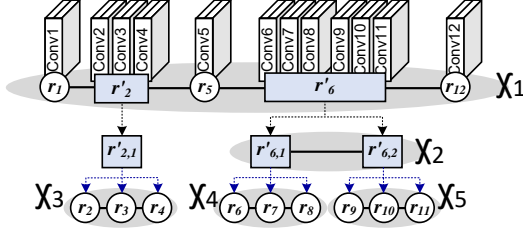


Figure 5. Hierarchical space generation (as an example of 12-layered network). There are 3 hierarchy level and five sub-spaces ($\mathcal{X}_1, \dots, \mathcal{X}_5$). The maximum space complexity is $\mathcal{O}(n^5)$ of \mathcal{X}_1 .

where i is the index of first layer in a group. Here, the range of rank in min-offset space is represented with the vector space and the t_i means the step size of vector space.

As an example, a 12-layered CNN is illustrated in Fig. 5. The maximum number of layers in a bottom group is set to 3, so that there are 3-hierarchical levels for layer grouping. The maximum space complexity is reduced from $\mathcal{O}(n^{12})$ to $\mathcal{O}(n^5)$ in \mathcal{X}_1 . At the top-level space, \mathcal{X}_1 is composed of 5 vector spaces, and we only retain the rank configurations that satisfy C_t in \mathcal{X}_1 . The sub-space \mathcal{X}_2 is defined by two vector spaces, which are also the grouped variables from the bottom layers in \mathcal{X}_4 and \mathcal{X}_5 . To simplify the extraction strategy, in our experiments, we choose the partial sets in each bottom sub-spaces ($\mathcal{X}_3, \mathcal{X}_4, \mathcal{X}_5$), by measuring the accuracy metric of each rank configuration.

5.4. Choice of Rank Configuration

Apart from the simple method described in Sec. 4, we use two methods, ENC-Model and ENC-Inf, for obtaining the optimal rank configuration for a given neural network. For both the methods, we prepare a subset \mathbf{R} using (14) including the candidate rank configurations.

In ENC-Model, we choose a rank configuration R_o that maximizes $A(R)$ which can be one of $A_m(R)$, $A_p(R)$, and $A_c(R)$ denoted in (5, 6, 7). I.e.,

$$R_o = \arg \max_R A(R) | R \in \mathbf{R}. \quad (17)$$

In ENC-Inf, we choose N rank configurations, which provide the largest values of $A(R)$. These N rank configurations are stored in \mathbf{R}_A and then evaluated over the validation dataset to choose a best rank configuration.

The complete process is given in Algorithm 1. The ENC-Map provides a quick and dirty solution, whereas ENC-Model and ENC-Inf approaches are relatively slower. However, even our slowest method easily outperforms state-of-the-art approaches in speed.

The proposed method can be used to reduce both the FLOPs and the memory consumption of a neural network. The constraint C_t can represent both the number of FLOPs or the number of parameters of the neural network. Also,

Algorithm 1 : Optimal Rank Configuration

INPUTS: $h \leftarrow$ A neural network, $C_t \leftarrow$ Target complexity, $method \leftarrow$ ENC-Map, ENC-Model, ENC-Inf

OUTPUT: $R_o \leftarrow$ Rank configuration

Parameters: $\delta_s \leftarrow$ Parameter for limiting the search space, $\delta_m \leftarrow$ Parameter for marginal error of C_t , $N \leftarrow$

Number of rank configurations for evaluation

//Layer-wise metrics

Compute $y_{p,l}, y_{m,l}$ for all $l \in 1 \dots L$

Compute f_{C-A}, f_{C-R}

if $method ==$ ENC-Map **then**

$R_o = f_{C-R}(C_t)$

else

//Candidate rank-set generation

$R_{max} = f_{C-R}(C_t + \delta_s)$

$R_{min} = f_{C-R}(C_t - \delta_s)$

$\mathbf{R} = \{\cup R \mid C_t - \delta_m < C(R) < C_t + \delta_m\}$
for $R \in [R_{min}, R_{max}]$

//Accuracy estimate for the

// whole neural network

Compute A of \mathbf{R}

if $method ==$ ENC-Model **then**

$R_o = \arg \max_R A(R)$ s.t. $R \in [R_{min}, R_{max}]$

else if $method ==$ ENC-Inf **then**

Compute $\mathbf{R}_A \in \mathbb{R}^{N \times L}$

Evaluate accuracy of each row of \mathbf{R}_A over the validation dataset

Select R_o from \mathbf{R}_A with best evaluation

end if

end if

our proposed methods can provide rank configurations under both complexity and accuracy constraints. Till now, the discussion followed complexity constrained systems. In other words, given a complexity constraint our aim is to obtain a rank configuration that maximizes the accuracy. However, shifting to accuracy constrained systems is straightforward. Given an accuracy constraint, we use the inverse mapping of f_{C-A}, f_{A-C} , to obtain the complexity corresponding to a given accuracy. The obtained complexity is input to Algorithm 1 to obtain the rank configuration.

6. Experimental Results

In this section, we present the experimental evaluation of the proposed methods. We first present a comparison of the proposed methods. We discuss the scenarios that dictate the choice of any of the proposed methods. Afterwards, we compare the proposed methods against some recently proposed neural-network optimizing methods.

For our experiments, we have optimized AlexNet [17], VGG-16 [26] and ResNet-56 [8] networks. For AlexNet and VGG-16, we have used the ImageNet [6] dataset. For

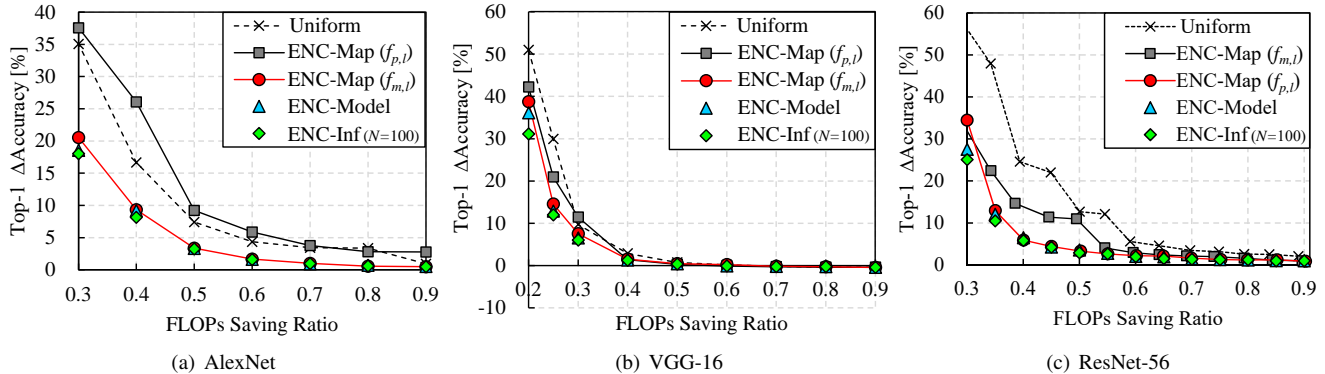


Figure 6. Performance comparison of overall accuracy metrics. Baseline top-1 accuracy is 56.6% for AlexNet, 70.6% for VGG-16, and 93.1% for ResNet-56. The results are without fine-tuning. Smaller Δ Acc. is better.

ResNet-56, we have used the Cifar-10 [16] dataset. We have performed the same pre-processing (image cropping and resizing) as described in the original papers [8, 17, 26]. Also, we have used 4% and 10% of the ImageNet and Cifar-10 training datasets as the validation datasets.

The parameters δ_s and δ_m were set to 10% of the original total complexity and 0.5% of the target complexity, respectively. For ENC-Model and ENC-Inf, we use the accuracy metric $A_m(R)$ for AlexNet, $A_c(R)$ for VGG-16, and $A_p(R)$ for ResNet-56 as $A(R)$. Also, note that we have performed channel decomposition to the first layer whenever required and spatial decomposition to the rest of the layers using truncated SVD. For VGG-16, the first layer was decomposed to half the original rank following [14] and for ResNet-56, the first layer was not compressed at all.

The experiments were conducted on a system with four Nvidia GTX 1080ti GPUs and an Intel Zeon E5-2620 CPU. The experiments conducted on the CPU used a single core and code optimization was not performed. The *Caffe* [13] library was used for development.

6.1. Comparison of Layer-wise accuracy metrics

This section presents the comparison of the two layer-wise accuracy metrics based on the results of the ENC-Map as shown in Fig. 6. We note that the PCA energy-based metric shows poor performance with the shallower AlexNet. This is expected as the PCA energy is not based on actual inference and expected to show poorer performance compared to the measurement-based layer-wise accuracy metric. However, with the deeper VGG-16 and ResNet-56, the performance of PCA energy-based and the measurement-based layer-wise accuracy metric is almost same. The reason is that the complexity difference from rank reduction on each layer is less as the layer is deeper, so that the accuracy difference is also smaller. The measurement-based metric can not completely represent the overall accuracy.

The PCA energy-based and measurement-based metrics

require 5 seconds and 5 minutes for ResNet-56. Note that once these metrics are evaluated, they can be used for different complexity constraints. For every new neural network that needs to be optimized, these metrics need to be evaluated beforehand.

6.2. Comparison of the Fast, Search without Inference, and Search with Inference Methods

In this section, we compare the performance of ENC-Map, ENC-Model and ENC-Inf against each other. In Fig. 6, it is seen that at lower compression (or relatively higher complexity requirements), the performance of all the three methods is almost the same. It means that the ENC-Map is the best solution at lower compression. At higher compression, the optimal rank configuration is more sensitive to the complexity and accuracy metric. Therefore, the performance of ENC-Map is lower than ENC-Model and ENC-Inf, and ENC-Inf using validation accuracy shows relatively the best performance. The time taken by each model is given in Table 1.

6.3. Performance Comparison with Other Methods

The overall results are summarized in Table 1. Here we use the decrease in accuracy (i.e. Δ Acc.), which is the difference of accuracy of the original and optimized neural networks, as a metric to evaluate different methods. Lower decrease in accuracy is desired. For a complexity metric, we use the percentage of $(1 - \text{compression ratio})$ as FLOPs. Also, we mention the results with uniform rank reduction, which applies the same rank reduction ratio to every layer of the neural network.

AlexNet with ImageNet. In [15], the authors show the compression results for FLOPs and parameters. It is not possible to use ENC-Map under both these constraints as it provides mapping only from one of these constraints to the accuracy. However, ENC-Model and ENC-Inf can be used by populating \mathbf{R} by rank configurations that sat-

Model	Target Complexity	Searching Policy	Top-1/Top-5 Δ Acc.[%]		Search Time
			w/o FT	w/ FT	
AlexNet (56.6% / 79.9%) @ImageNet	FLOPs 37.5% Parameters 18.4% [15]	Y-D <i>et al.</i> [15]	- / -	- / 1.6	-
		ENC-Inf	- / -	-0.1 / -0.2	3m @4GPUs
		ENC-Model	- / -	-0.1 / -0.2	1m @CPU
VGG-16 (70.6% / 89.9%) @ImageNet	FLOPs 25%	Uniform	29.9 / 23.6	0.8 / 0.5	-
		Heuristic [9]	- / 11.7	- / -	-
		ADC [9]	- / 9.2	- / -	4h @8GPUs
		ARS [14]	13.0 / 9.1	-0.3 / -0.1	7h @4GPUs (in our impl.)
		ENC-Inf	10.7 / 7.3	-0.6 / -0.2	5m @4GPUs
		ENC-Model	11.3 / 7.9	-0.7 / -0.2	3m @CPU
ResNet-56 (93.1% / -) @Cifar-10	FLOPs 50%	ENC-Map	14.5 / 10.2	-0.2 / -0.1	4s @CPU
		Uniform	12.7 / -	0.2 / -	-
		AMC [10]*	2.7* / -	0.9* / -	1h @GPU
		ENC-Inf	2.9 / -	0.1 / -	3m @4GPUs
		ENC-Model	3.5 / -	0.1 / -	1m @CPU
		ENC-Map	3.3 / -	0.1 / -	3s @CPU

Table 1. Performance comparison of network compression techniques. The proposed methods, uniform, [9], heuristic in [9], and [14] use the SVD based spatial decomposition. [15] uses the Tucker decomposition based channel decomposition. [10] uses the channel pruning. Baseline accuracy of [10]* is 92.8%. Smaller Δ Acc. is better.

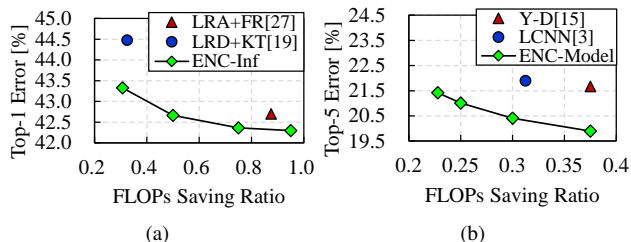


Figure 7. Performance comparison for AlexNet. (a) compression of only convolutional layers. (b) compression of whole layers including fully-connected layers. Smaller error is better.

isfy both the FLOPs and parameters constraints. We have used $N=50$ here and optimize both convolutional and fully-connected layers. Initial learning rate of 10^{-3} was used, which was reduced by a factor of 2 after every 2 epochs till the 16-th. Fine-tuning takes around 9 hours. As denoted in Table 1, our method shows 1.8% higher top-5 accuracy than [15] at the same complexity. To find the rank configuration, our algorithm only takes only a minute with a single core CPU with ENC-Model and 3 minutes on 4 GPUs with ENC-Inf. Fig. 7 indicates that our method outperforms the state-of-the-art. The FLOPs saving ratios of reffed works in Fig. 7 are calculated in our experiment. We achieve 43.33% and 42.40% top-1 error at 30.7% and 95.0% FLOPs for Fig. 7(a). Also, we attain the 20.4% top-5 error at 30% FLOPs for Fig. 7(b). Compared to [19, 27] using the accuracy compensation techniques such as knowledge transfer [19] and force regularization [27], our method uses only fine-tuning which is the most simple and effective strategy.

VGG-16 (FLOPs 20%)	Top-5 Δ Acc.	Search Range
Asym.3D [28]	1.0%	
Y-D <i>et al.</i> [15]	0.5%	Layer-by-layer
CP-3C [11]	0.3%	
ENC-Inf	0.0%	Whole-network

Table 2. Comparison over target complexity of 20% FLOPs with VGG-16. Baseline top-5 accuracy is 89.9%.

VGG-16 with ImageNet. We optimize the convolutional layers under a FLOPs constraint. The complexity constraint is set to 25% and 20% FLOPs to compare with [9, 14] and [11, 15, 28], respectively. For ENC-Inf, we set $N=40$. The layers 7-8, 9-10, and 11-13 are grouped each other for top-level sub-spaces. The compressed network was fine-tuned with an initial learning rate of 10^{-5} , which was decreased by a factor of 10 at the fourth epoch. Fine-tuning takes about 1 day. With 25% FLOPs reduction, ENC-Inf takes only 5 minutes at 4 GPUs, and it shows the 2.3% and 0.3% higher top-1 accuracy without and with fine-tuning, respectively, compared to [14]. As denoted in Table 1, our ENC-Map is extremely fast. It can find the result in only 4 seconds with a single core CPU, while the previous research takes 4 hours at 8 GPUs [9] and 7 hours at 4 GPUs [14]. Results with 20% FLOPs reduction are given in Table 2. It is seen that our method outperforms the layer-by-layer strategies.

Model	Searching Policy	FLOPs	Top-1 Δ Acc.
AlexNet	ENC-Inf	31%	0.0%
VGG-16	ENC-Model	24%	-0.4%
ResNet-56	ENC-Map	55%	-0.1%

Table 3. Lossless compression with full fine-tuning.

Searching Policy	Fine-tuning Epochs	FLOPs	Top-1 Δ Acc.
ADC [9]	0	64%	0.0%
ENC-Model	0	57%	-0.1%
	0.1	41%	-0.1%
ENC-Model	0.2	39%	-0.1%
	1	33%	0.0%

Table 4. Fast lossless compression with brief fine-tuning for VGG-16. Baseline top-1 accuracy is 70.6%. Smaller Δ Acc. is better.

ResNet-56 with Cifar10. The search space is defined in 3-level hierarchy. The layers 2-19, 21-37, and 39-55 are placed in separated groups excluding first convolutional layer and fully-connected layer. We set the the maximum number of bottom layers in a group as four. The second-level spaces are defined by the number of bottom layers such as Fig. 5. For ENC-Inf, we set $N=20$. The compressed ResNet-56 is fine-tuned with an initial learning rate of 10^{-3} , which is reduced by a factor of 10 at the 16th, 24th and 32nd epoch. Fine-tuning takes around 1 hour. ENC-Map and ENC-Model achieve a 0.1% accuracy loss (i.e. 93.1% top-1 accuracy) with 50% FLOPs reduction after fine-tuning. The times taken by ENC-Map and ENC-Inf are 3 seconds with single core CPU and 5 minutes with 4 GPUs, respectively. It is much more efficient compared to the learning based state-of-the-art, which takes 1 hour on a single GPU [10].

6.4. Lossless Compression

The idea of lossless compression is to set the target accuracy to that of the original neural network and then optimize the network. However, since we use fine-tuning after optimization, we can set the target accuracy to slightly lower than that of the original neural network. The remaining accuracy is recovered by fine-tuning. To set the reduced accuracy constraint, we use the accuracy estimation method in [14]. Then, the complexity constraint (i.e. FLOPs) is calculated from the mapping function between the accuracy and complexity constraints. As summarized in Table 3, our compression methods achieve a significant reduction in FLOPs without accuracy loss.

The combination of our fast compression method and brief fine-tuning can further reduce the FLOPs without accuracy loss. Table 4 shows the result of lossless compression

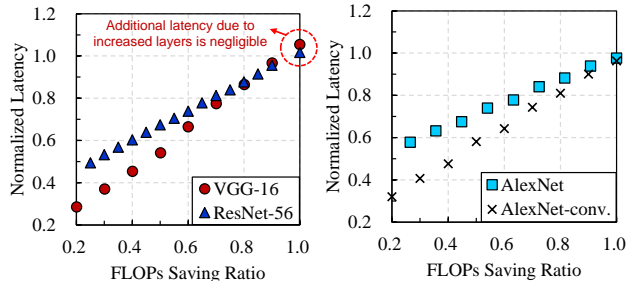


Figure 8. Normalized CPU latency of optimized models. The latency of baseline CNN is 10.59s in VGG-16, 142.2ms in ResNet-56, and 825.0ms in AlexNet for single image classification.

sion with fine-tuning under 1 epoch. The accuracy thresholds considering fine-tuning are calculated for 0.1, 0.2, and 1 epochs using the method in [14]. We reduced the FLOPs by 41% with VGG-16 without any accuracy loss. The process took only 0.1 epoch or 22 minutes with a single GPU. Also, our method with 1 epoch fine-tuning takes 3.7 hours with a single GPU, and it provides better compression (33% FLOPs) compared to the 4 hour search (64% FLOPs) in [9].

6.5. Results on an Embedded Board

We evaluate the latency of the compressed network models for inference on the ODROID-XU4 board with Samsung Exynos5422 mobile processor. Fig. 8 shows that the FLOPs saving ratio in our paper is directly related to the real latency for single image inference. We use ENC-Model for optimizing the convolutional layers of AlexNet, VGG-16, and ResNet-56 in Fig. 8. We note that the latency of convolutional layers is 72% and 62% of total latency for the baseline ResNet-56 and AlexNet, respectively, and the bias latency in Fig. 8 is due to the other operations including batch normalization and fully-connected layers. The results of AlexNet-conv indicate that the theoretical FLOPs reduction of convolutional layers corresponds to the latency improvement of those layers.

7. Conclusion

In this paper, we propose the efficient neural network compression methods. Our methods are based on low-rank kernel decomposition. We propose a holistic, model-based approach to obtain the rank configuration that satisfies the given set of constraints. Our method can compress the neural network while providing competitive accuracy. Moreover, the time taken by our method for compression is in seconds or minutes, whereas previously proposed methods take hours to achieve similar results.

Acknowledgement This work was supported by MSIT as GFP / (CISS-2013M3A6A6073718).

References

- [1] Anubhav Ashok, Nicholas Rhinehart, Fares Beainy, and Kris M Kitani. N2n learning: Network to network compression via policy gradient reinforcement learning. Apr 2018.
- [2] Marcella Astrid and Seung-Ik Lee. Cp-decomposition with tensor power method for convolutional neural networks compression. In *Big Data and Smart Computing (BigComp), 2017 IEEE International Conference on*, pages 115–118. IEEE, 2017.
- [3] Hessam Bagherinezhad, Mohammad Rastegari, and Ali Farhadi. Lcnn: Lookup-based convolutional neural network. In *Proceedings of the IEEE Conference on Computer Vision and Pattern Recognition*, pages 7120–7129, 2017.
- [4] Han Cai, Tianyao Chen, Weinan Zhang, Yong Yu, and Jun Wang. Reinforcement learning for architecture search by network transformation. *arXiv preprint arXiv:1707.04873*, 2017.
- [5] Ting-Wu Chin, Cha Zhang, and Diana Marculescu. Layer-compensated pruning for resource-constrained convolutional neural networks. *arXiv preprint arXiv:1810.00518*, 2018.
- [6] Jia Deng, Wei Dong, Richard Socher, Li-Jia Li, Kai Li, and Li Fei-Fei. Imagenet: A large-scale hierarchical image database. In *Computer Vision and Pattern Recognition, 2009. CVPR 2009. IEEE Conference on*, pages 248–255. IEEE, 2009.
- [7] Misha Denil, Babak Shakibi, Laurent Dinh, Nando de Freitas, et al. Predicting parameters in deep learning. In *Advances in Neural Information Processing Systems (NIPS)*, pages 2148–2156, 2013.
- [8] Kaiming He, Xiangyu Zhang, Shaoqing Ren, and Jian Sun. Deep residual learning for image recognition. In *Proceedings of the IEEE conference on computer vision and pattern recognition*, pages 770–778, 2016.
- [9] Yihui He and Song Han. Adc: Automated deep compression and acceleration with reinforcement learning. *arXiv preprint arXiv:1802.03494*, 2018.
- [10] Yihui He, Ji Lin, Zhijian Liu, Hanrui Wang, Li-Jia Li, and Song Han. Amc: Automl for model compression and acceleration on mobile devices. In *Proceedings of the European Conference on Computer Vision (ECCV)*, pages 784–800, 2018.
- [11] Yihui He, Xiangyu Zhang, and Jian Sun. Channel pruning for accelerating very deep neural networks. In *International Conference on Computer Vision (ICCV)*, volume 2, 2017.
- [12] Max Jaderberg, Andrea Vedaldi, and Andrew Zisserman. Speeding up convolutional neural networks with low rank expansions. *arXiv preprint arXiv:1405.3866*, 2014.
- [13] Yangqing Jia, Evan Shelhamer, Jeff Donahue, Sergey Karayev, Jonathan Long, Ross Girshick, Sergio Guadarrama, and Trevor Darrell. Caffe: Convolutional architecture for fast feature embedding. In *Proceedings of the 22nd ACM international conference on Multimedia*, pages 675–678. ACM, 2014.
- [14] Hyeji Kim and Chong-Min Kyung. Automatic rank selection for high-speed convolutional neural network. *arXiv preprint arXiv:1806.10821*, 2018.
- [15] Yong-Deok Kim, Eunhyeok Park, Sungjoo Yoo, Taelim Choi, Lu Yang, and Dongjun Shin. Compression of deep convolutional neural networks for fast and low power mobile applications. In *Proceedings of the International Conference on Learning Representations (ICLR)*, May 2016.
- [16] Alex Krizhevsky and Geoffrey Hinton. Learning multiple layers of features from tiny images. Technical report, Cite-seer, 2009.
- [17] Alex Krizhevsky, Ilya Sutskever, and Geoffrey E Hinton. Imagenet classification with deep convolutional neural networks. In *Advances in neural information processing systems*, pages 1097–1105, 2012.
- [18] Hao Li, Asim Kadav, Igor Durdanovic, Hanan Samet, and Hans Peter Graf. Pruning filters for efficient convnets. *arXiv preprint arXiv:1608.08710*, 2016.
- [19] Shaohui Lin, Rongrong Ji, Chao Chen, Dacheng Tao, and Jiebo Luo. Holistic cnn compression via low-rank decomposition with knowledge transfer. *IEEE transactions on pattern analysis and machine intelligence*, 2018.
- [20] Shaohui Lin, Rongrong Ji, Xiaowei Guo, Xuelong Li, et al. Towards convolutional neural networks compression via global error reconstruction. In *IJCAI*, pages 1753–1759, 2016.
- [21] Shaohui Lin, Rongrong Ji, Yuchao Li, Yongjian Wu, Feiyue Huang, and Baochang Zhang. Accelerating convolutional networks via global & dynamic filter pruning. In *IJCAI*, pages 2425–2432, 2018.
- [22] Hanxiao Liu, Karen Simonyan, Oriol Vinyals, Chrisantha Fernando, and Koray Kavukcuoglu. Hierarchical representations for efficient architecture search. *arXiv preprint arXiv:1711.00436*, 2017.
- [23] Jian-Hao Luo, Jianxin Wu, and Weiyao Lin. Thinet: A filter level pruning method for deep neural network compression. *arXiv preprint arXiv:1707.06342*, 2017.
- [24] Shinichi Nakajima, Masashi Sugiyama, S Derin Babacan, and Ryota Tomioka. Global analytic solution of fully-observed variational bayesian matrix factorization. *Journal of Machine Learning Research*, 14(Jan):1–37, 2013.
- [25] Esteban Real, Alok Aggarwal, Yanping Huang, and Quoc V Le. Regularized evolution for image classifier architecture search. *arXiv preprint arXiv:1802.01548*, 2018.
- [26] Karen Simonyan and Andrew Zisserman. Very deep convolutional networks for large-scale image recognition. In *Proceedings of the International Conference on Learning Representations (ICLR)*, May 2015.
- [27] Wei Wen, Cong Xu, Chunpeng Wu, Yandan Wang, Yiran Chen, and Hai Li. Coordinating filters for faster deep neural networks. In *Proceedings of the IEEE International Conference on Computer Vision*, pages 658–666, 2017.
- [28] Xiangyu Zhang, Jianhua Zou, Kaiming He, and Jian Sun. Accelerating very deep convolutional networks for classification and detection. *IEEE transactions on pattern analysis and machine intelligence*, 38(10):1943–1955, 2016.